

Real-Time Performance of OPC UA

Erkin Kirdan
Framatome
erkin.kirdan@framatome.com

Filip Rezabek
Technical University of Munich
filip.rezabek@tum.de

Nikolas Mühlbauer
Technical University of Munich
n.muehlbauer@tum.de

Georg Carle
Technical University of Munich
carle@tum.de

Marc-Oliver Pahl
IMT Atlantique
marc-oliver.pahl@imt-atlantique.fr

Abstract—OPC UA is an industry-standard machine-to-machine communication protocol in the Industrial Internet of Things. It relies on time-sensitive networking to meet the real-time requirements of various applications. Time-sensitive networking is implemented through various queuing disciplines (qdiscs), including Time Aware Priority, Multiqueue Priority, Earliest TxTime First, and Credit-Based Shaper. Despite their significance, prior studies on these qdiscs have been limited to a few. They have often been confined to point-to-point network topologies using proprietary software or specialized hardware. This study builds upon existing research by evaluating all these qdiscs in point-to-point and bridged topologies using open-source software on commercial off-the-shelf hardware. We first identify the optimal configuration for each qdisc and then compare their jitter, latency, and reliability through experiments. Our results show that open-source OPC UA on commercial off-the-shelf hardware can effectively meet the stringent real-time requirements of many industrial applications and provide a foundation for future research and practical deployments.

Index Terms—Experiments, OPC UA, TSN

I. INTRODUCTION

Open Platform Communications (OPC) Unified Architecture (UA) is a machine-to-machine communication protocol for industrial automation developed by the OPC Foundation [1]. With its platform-independent design, OPC UA offers an efficient and secure framework for interoperability between different systems and devices. It supports complex data types and object models, making it versatile for various industrial applications. OPC UA ensures security measures, including encryption, authentication, and authorization, to safeguard against unauthorized access and cyber threats in critical infrastructures. Its ability to integrate with different hardware and software and its support for client-server and publisher-subscriber communication models makes OPC UA a key enabler for the Industrial Internet of Things.

By integrating Time Sensitive Networking (TSN), OPC UA meets industrial processes' stringent timing and reliability requirements, ensuring synchronized and timely communication between devices and systems. This integration is pivotal for supporting real-time operations in Industry 4.0, where precise timing and coordination across diverse components are essential.

TSN is a set of IEEE standards developed to improve the reliability and determinism of standard Ethernet networks.

It enables the precise timing and synchronization of data packets across a network, ensuring low latency and minimal jitter. TSN incorporates features like time synchronization, traffic scheduling, and resource reservation, allowing for the coexistence of regular and time-critical traffic on the same network.

Despite the crucial role of real-time communication in OPC UA field devices [2], there needs to be more research that explores the capabilities of open-source OPC UA on commercial off-the-shelf (COTS) hardware. The current studies primarily rely on specialized hardware and propriety software. They examine a limited number of queuing disciplines (qdiscs), preventing a comprehensive comparison and identification of the optimal configuration for various requirements.

Our research aims to answer the following questions:

Q1: How does open-source OPC UA perform on COTS hardware?

Q2: How do various qdiscs affect performance?

Q3: How does the presence of a bridge and cross-traffic affect performance?

Q4: What is the optimal configuration for each qdisc?

To determine the real-time performance of OPC UA over TSN, we conduct reproducible experiments to measure reliability as packet drop rate, latency as round trip time (RTT), and jitter, which are relevant metrics as outlined in the TSN methodology [3]. We determine the optimal configuration for a given setup through an iterative investigation of different parameter values. The experiments are conducted on two point-to-point (P2P) setups with different hardware capabilities and a bridged setup involving a Linux switch.

Real-time applications have different requirements of reliability, latency, and jitter [4]. Our study encompasses relevant use cases, such as tactile interaction, safety monitoring and control alarms, automated guide vehicles, smart grid protection, and motion control. Among these, motion control demands the most stringent requirements, such as a maximum latency of 0.1 ms, maximum jitter of 0.05 ms, and 99.999% reliability [4]. Our results show that the open-source OPC UA on COTS hardware meets such requirements.

$\geq 1\text{B}$	11 B	$1 + 2n\text{B}$	$\geq 10\text{B}$	variable
header _m	header _g	header _p	header _e	payload

Fig. 1: UADP message structure [1]

II. BACKGROUND

This section provides the background of our research, starting with OPC UA publish-subscribe (PubSub). Related to TSN, we focus on Precision Time Protocol (PTP) [5], IEEE 802.1Qav [6], and IEEE 802.1Qbv [7] with their corresponding Linux implementations.

A. OPC UA PubSub

In 2018, the OPC foundation introduced the PubSub extension as part of the OPC UA specification [1]. OPC UA PubSub encompasses three communication parties. A publisher sends messages to subscribers through a middleware. While the PubSub protocol does not specify the middleware itself, it relies on underlying protocols for its operation. Additionally, OPC UA PubSub enables encryption and signing of the messages, which are critical for security.

The exchanged messages, *NetworkMessage*, consist of a header and payload organized into *DataSetMessages*. Each *DataSetMessage* contains a *DataSet*, which is not parsable or included in the message but must be known by the subscriber. To address this, metadata, including field names and data types, is introduced to provide a clear understanding of the *DataSet*. This metadata can be obtained through server/client OPC UA or using special mechanisms offered by OPC UA PubSub. The metadata version is an integral part of the *DataSetMessage* to ensure that the publisher and subscriber understand the exchanged messages.

OPC UA PubSub messages can be mapped to JSON or binary Unified Architecture Datagram Protocol (UADP). While JSON is a standard format for data representation, it is not intended for real-time communication. Therefore, OPC UA PubSub introduces a new application layer protocol named UADP, which offers a unique message structure. Figure 1 depicts the structure of UADP without security headers.

The message header, denoted as *header_m*, is a mandatory component of the communication protocol. On the other hand, the group header *header_g*, payload header *header_p*, and extended header *header_e* are optional components. The main header holds information such as the protocol version, flags, the publisher’s unique identifier, and the class of *DataSet*. The group header, in turn, includes the message and sequence numbers, while the extended header includes a timestamp. The optional payload header encodes the ID of the *DataSetWriter*, allowing subscribers to identify the message’s origin and the content of the *DataSet*. It is important to note that the header is not encrypted, enabling subscribers to filter out unwanted messages. The structure of encrypted and signed messages is illustrated in Figure 2.

UADP operates as an application layer protocol. It can be deployed on top of the following protocols:

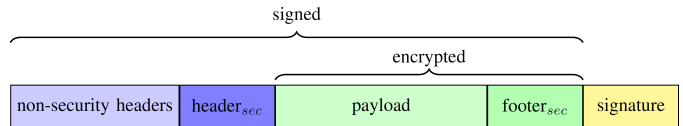


Fig. 2: UADP security [1]

- Ethernet (layer 2),
- User Datagram Protocol (UDP) (layer 4),
- Advanced Message Queuing Protocol, or Message Queuing Telemetry Transport (MQTT) (application layer).

The implementation of OPC UA PubSub varies based on the underlying protocol. For instance, where MQTT is the underlying protocol, OPC UA PubSub uses brokers. Alternatively, when UDP or Ethernet is used, OPC UA PubSub operates brokerless. Additionally, OPC UA PubSub is compatible with TSN when deployed with Ethernet. Due to the support of TSN, we focus only on brokerless OPC UA over Ethernet.

OPC UA over Ethernet is identified by the `EtherType 0xb62c` and encapsulates UADP messages directly, bypassing the need for network or transport layer headers. The addressing format for OPC UA over Ethernet follows the pattern of `opc.eth://host[:VLAN ID[.VLAN priority]]`. The host component can be a hostname, a Media Access Control (MAC) address, or an Internet Protocol (IP) address. When specifying a MAC address, the bytes should be separated by hyphens instead of colons. It is important to note that IP addresses and hostnames must be resolved to corresponding MAC addresses before communication.

The `open62541` project¹ is the most widely used open-source implementation of OPC UA [8] and the only one that supports the PubSub protocol over TSN [9]. It includes an OPC UA stack, a server, a client software development kit, and the implementation of OPC UA PubSub. The application supports JSON or UADP encoding over Ethernet or UDP.

With raw Ethernet as its underlying protocol, OPC UA PubSub supports TSN. Since being released before integrating the Time-Aware Priority Shaper (TAPRIO) qdisc into the Linux kernel, the application implements the IEEE 802.1Qbv standard in software. The PubSub setup requires two hosts: the publisher **P** and loopback **L**. The OPC UA server periodically retrieves and increments variables using an *application thread*. Additionally, two supplementary threads are responsible for publishing and subscribing. The **L** application subscribes to **P**, storing the subscribed values within its OPC UA server.

A configurable cycle time *c* defines the duration of a cycle, which corresponds to the TAPRIO cycle time. The publish and subscribe applications begin their cycles at full seconds. At $0.4c$ before the start of the next cycle time, the publisher thread is activated and initiates publication. The transmission time is set to the start of the next cycle time plus a configurable offset *o*. Figure 3 illustrates the starting time of each thread and the offset relative to the cycle time. The subscriber thread is executed at the start of the cycle ($0.0c$). At $0.3c$, the user thread

¹<https://github.com/open62541/open62541>

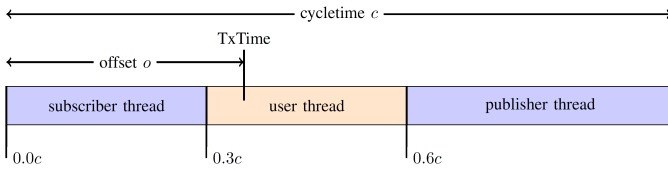


Fig. 3: Overview of one cycle time

stores the values received by the subscriber in the OPC UA address space of the loopback host or increments the variables in the publisher host. At $0.6c$, $0.4c$ before the start of the next cycle, the publisher thread is again activated, and the execution follows as described above.

B. Time Synchronization

PTP is crucial for synchronous TSN standards, such as the IEEE 802.1Qbv. It synchronizes individual physical clocks on various hops in high precision.

The Linux PTP project² encompasses the tools *ptp4l*³, *phc2sys*⁴, and *pmc*⁵. The *ptp4l* tool, a command-line utility, implements the PTP standard IEEE 1588 [5] and can operate over Ethernet, IPv4, or IPv6 networks. The *ptp4l* daemon must run on all interfaces to synchronize the system's clocks and identify the PTP Grandmaster Clock (GM), which serves as the reference time for the entire system organized in a master-slave hierarchy. The *phc2sys* tool synchronizes the clocks within a single system and can run in automatic mode, utilizing information from the *ptp4l* daemon to achieve synchronization. Hardware timestamping can be leveraged to achieve nanosecond-level precision when utilizing a Network interface card (NIC) that supports IEEE 802.1AS, such as the commercially available Intel[®] I210 NIC.

C. Linux Traffic Control

We provide an overview of the Linux TSN implementations based on the details described in the IEEE standards. Within the scope of this paper, we focus on the Multiqueue Priority (MQPRIO) and TAPRIO qdiscs as parents and the Earliest Time First (ETF) and Credit-Based Shaper (CBS) qdiscs as children, specifically in the context of TSN.

The IEEE 802.1Qav standard outlines two algorithms for shaping and prioritizing network traffic. The first algorithm, strict priority forwarding, prioritizes traffic based on class priority, with higher priority classes transmitted first. This algorithm is already specified in the IEEE 802.1Q standard [10]. As part of IEEE 802.1Qav, it is considered a TSN algorithm. If no packets are in the higher priority class, lower priority packets are transmitted. This algorithm is implemented with the MQPRIO qdisc⁶. qdiscs handles traffic and is organized in a parent-child hierarchy. Relevant parameters are `num_tc`, which indicates the number of configured traffic classes, and

TABLE I: PCP to TC mapping according to IEEE 802.1Qav

PCP	0	1	2 (SR-B)	3 (SR-A)	4	5	6	7
TC	1	0	6	7	2	3	4	5

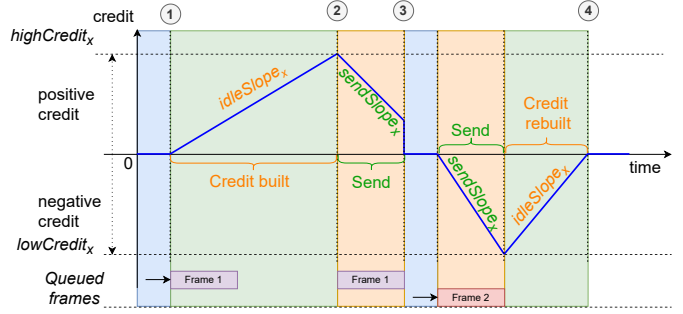


Fig. 4: Credit of CBS over time, based on [3], [6]

map, which maps packet priorities to corresponding traffic classes. The second algorithm defined by IEEE 802.1Qav is the CBS algorithm. Bridges implementing IEEE 802.1Qav should prioritize CBS traffic classes over those using strict priority forwarding, as indicated by the default Priority Code Point (PCP) to traffic control (tc) mapping in Table I.

The CBS qdisc⁷ regulates and secures bandwidth allocation for a specific traffic class. It is implemented as a child qdisc in conjunction with a root qdisc, such as MQPRIO, which performs traffic classification. Figure 4 shows the credit lifecycle with the four CBS parameters - $highCredit_x$, $lowCredit_x$, $idleSlope_x$, and $sendSlope_x$. The first two define the maximum and minimum allowed credit. $idleSlope_x$ marks the credit replenishment rate, and $sendSlope_x$ the credit spending rate. Once a frame arrives, the credit starts to build up ①. After the $highCredit_x$ is reached ②, the frame is sent after non-policed frames are transmitted, following the $sendSlope_x$ parameter. If no further frames are in the queue, the credit drops to 0, ③. If there is still some credit from $sendSlope_x$, the next frame gets sent out immediately. This triggers the credit rebuilt since the credit is fully depleted, ④. It is worth mentioning that the parameters in CBS are defined in bits or bits per second, as specified by the IEEE 802.1Qav standard, as opposed to bytes or kilobits per second in Linux.

In 2015, IEEE published the IEEE 802.1Qbv standard, which provides enhancements for scheduled traffic. With the implementation of IEEE 802.1Qbv, it is possible to implement a Time-Division Multiple Access scheme for Ethernet networks. Each traffic class has a queue with an associated *gate*, which can be opened or closed anytime. Packets can only be dequeued from a queue when its gate is open. The gates are controlled by a schedule consisting of gate operation instructions. Each operation specifies a gate configuration and the duration for which the configuration remains valid. The operations are executed in sequence, taking into account the specified intervals. This process is repeated to form a cycle,

²<https://sourceforge.net/projects/linuxptp/>

³<https://linux.die.net/man/8/ptp4l>

⁴<https://linux.die.net/man/8/phc2sys>

⁵<https://linux.die.net/man/8/pmc>

⁶<https://man7.org/linux/man-pages/man8/tc-mqprio.8.html>

⁷<https://man7.org/linux/man-pages/man8/tc-cbs.8.html>

with the cycle time equal to the sum of all the intervals in the schedule.

The TAPRIO qdisc⁸, also known as the Time-Aware Shaper (TAS), is designed to calculate schedules with time slots for different traffic classes as specified in the IEEE 802.1Qbv standard. Like the MQPRIO qdisc, packets are initially mapped to traffic classes and Tx queues. To synchronize schedules across all network devices, it is necessary to correctly set the `base-time` and ensure its alignment among all hosts. As a result, TAPRIO falls under synchronous TSN standards. The base-time is specified in nanoseconds and indicates the starting point of the schedule. The `sched-entry` parameters follow and define the gate state and its duration. The syntax is `sched-entry S $MASK $DURATION`, where `$DURATION` represents the time window duration, and `$MASK` indicates which gate is open or closed during that window. To avoid interference between windows, guard windows can be added between them, with the guard window size computed based on the packet serialization time, packet size, and link speed. The cycle time is the sum of all schedule entries, including the guard windows. The `flags` support TxTime mode (`flags 0x1`) and full offload mode (`flags 0x2`). The TxTime mode sets the packet's TxTime and uses the ETF qdisc to control when a packet is transmitted. The `txtime-delay` value is required when the flags are set to `0x1` and serves as a delay to compensate for system delay. It should be set to a value greater than the δ value of the ETF qdisc.

The ETF qdisc is employed when a packet is transmitted at a specific TxTime⁹. This feature, the *LaunchTime*, is illustrated in Figure 5. In Figure 5a, a packet with priority three and TxTime T arrives at the root qdisc for further processing. In Figure 5b, the packet is classified based on its priority to a given class and corresponding child qdisc queue. The packet is dequeued at time δ before the TxTime to the ring buffer, where it is taken to the NIC, Figure 5c. At the TxTime, the packet is eventually dequeued to the wire, as shown in Figure 5d.

As shown in the example, ETF can be utilized as a child qdisc with MQPRIO or mainly with the TAPRIO as the parent qdisc. It is especially crucial for the TAPRIO qdisc, as the packets could only be appropriately dequeued within their respective windows with it. The TxTime for a packet is specified in the SKB `SO_TXTIME` option. If packets arrive at the queue after their designated TxTime, they are dropped by the NIC. The ETF qdisc sorts packets based on their TxTime, and at a configurable offset δ before the TxTime, the qdisc dequeues the packet for transmission to the NIC. The offset δ can also compensate for system delay. If the NIC supports the *LaunchTime* feature, the ETF can be offloaded for improved performance.

Linux has the `tc` command line tool to manage the con-

figuration of the qdiscs in the networking stack¹⁰. The traffic packet priorities are mapped to traffic classes corresponding to one or more Tx queues. The Tx queue with the lowest number is emptied first. The Intel[®] I210 NIC, for example, has four hardware queues, each of which can have its child qdisc configured. The first qdisc corresponds to hardware queue one and is assigned the highest traffic priority. Priorities are stored in the Linux socket buffer (SKB) and correspond to their VLAN PCP header field, as described in [11]. If a NIC supports the respective standards, the algorithms can be offloaded, potentially resulting in a processing speedup.

III. RELATED WORK

Two similar related works [11] and [12] employ OPC UA PubSub to establish communication between two P2P connected devices, utilizing the Intel[®] I210 NIC and the open-source *open62541* stack. In [11], the TAPRIO cycle time is set to $100\mu\text{s}$, while in [12], it is set to $200\mu\text{s}$. Our experiments use a cycle time of $250\mu\text{s}$, which is determined by the system performance. Section V-A outlines determining the optimum cycle time value and other related parameters.

Research by Eckhardt et al. [13] utilizes specialized embedded hardware for TSN instead of COTS hardware. The OPC UA software stack is not specified. TAS is preferred without providing any information regarding the implementation. In contrast to our study, [13] is configured with shorter cycle times for TAS than for the application. Moreover, it uses software timestamps, which reduce the accuracy of measurements but allow the investigation of application bottlenecks.

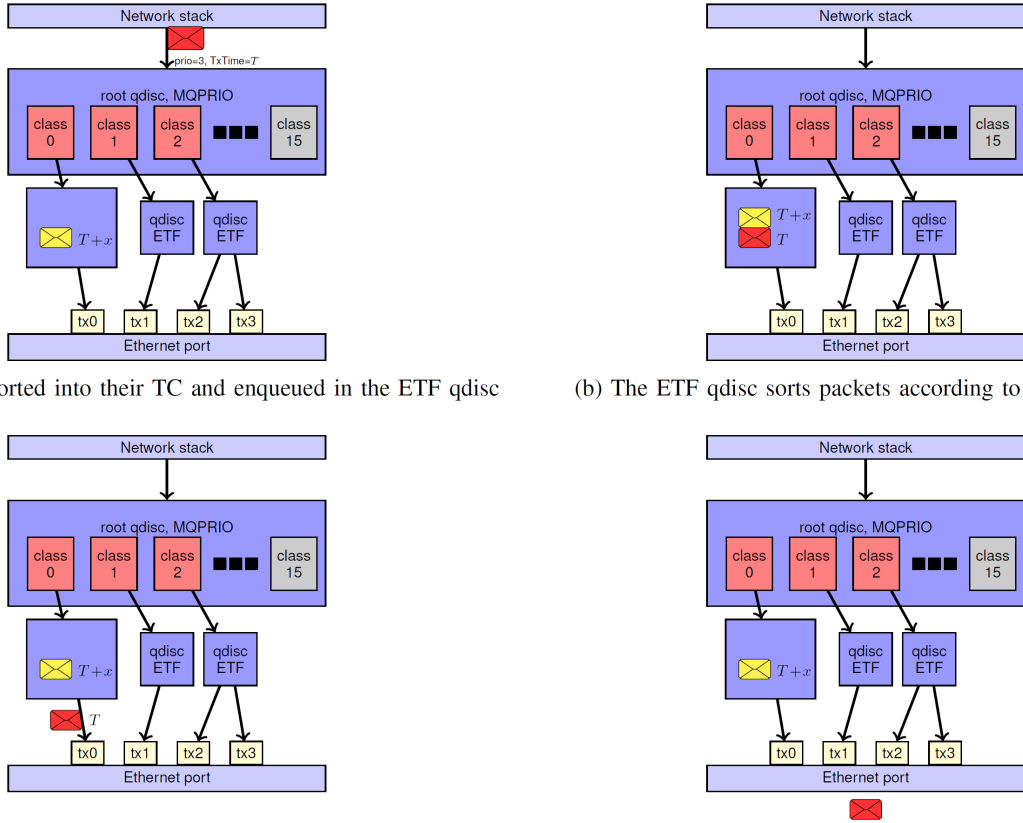
A study by Farzaneh et al. [14] conducts TAS experiments using cyclic real-time traffic with a cycle time of $500\mu\text{s}$. The setup employs commercial switches with a TAS implementation in a field programmable gate array and uses three sequentially connected switches. However, since the end devices lack hardware timestamping, the timestamps of the adjacent switch ports are utilized. The traffic is unidirectional, with the first switch acting as the source and the second as the sink. In contrast, our study uses a loopback application on the second host and mirrors the messages to their origin, allowing for the RTT analysis. In our research, we also employ MQPRIO, the Linux implementation of strict priority forwarding, to perform experiments with priority forwarding, similar to the approach taken by [14].

Li et al. [15] investigate a bridged TAS network utilizing two specialized TSN switches and hardware TSN modules to enable TSN on end devices. However, the setup relies solely on commercial hardware, contrasting our approach. A cycle time of 20ms is used, and all TSN traffic is transmitted in a single direction. The implementation has OPC UA with a server/client communication pattern instead of PubSub. Only the client is open-source. The study does not include the jitter or packet drop rate measurements. Although the implementation achieves bounded latency using TAS, the bound is

⁸<https://man7.org/linux/man-pages/man8/tc-taprio.8.html>

⁹<https://man7.org/linux/man-pages/man8/tc-ETF.8.html>

¹⁰<https://linux.die.net/man/8/tc>



(a) Packets get sorted into their TC and enqueued in the ETF qdisc

(b) The ETF qdisc sorts packets according to their TxTime

(c) At δns before the TxTime, the ETF qdisc hands over packets to the NIC

(d) The NIC sends the packet at TxTime according to its hardware clock

Fig. 5: Linux Traffic Control at the example of MQPRIO and ETF

almost 900 μs , significantly higher than the average latency of approximately 40 μs without TAS.

A study by Gogolev et al. [16] investigates the performance of TAS switches based on proprietary software using specialized evaluation hardware. The approach utilizes the OPC UA server and client to perform read or write requests at varying intervals. However, unlike our TAS configuration, the work does not examine worst-case RTT, jitter, or packet drop, focusing solely on average RTT. A subsequent study by the same authors [17] combines TAS with CBS to limit bandwidth for best-effort (BE) traffic. The findings reveal that the impact of TAS is more significant than that of CBS.

Arestova et al. [18] research focuses on the *glstaprio* framework and experiments on a two-node network. The experiments analyze the performance of a one-way data flow from a sender to a receiver. The sender uses a specialized TSN NIC from Kontron, and the receiver uses an Intel[®] I210 NIC to capture hardware timestamps. Our work shares the same OPC UA PubSub implementation as [18], *open62541*, and uses a 1 ms cycle time with a 100 μs priority traffic window.

An evaluation by Gruener et al. [19] uses OPC UA PubSub over TSN on COTS hardware. Similarly, like [11], it relies on the *open62541* stack. Concerning network size, the evaluation only considers measurements in P2P topology using Intel[®] I350 NIC that supports PTP. The setup uses the real-time

kernel on one of the hosts to limit operating system noise. Since the NIC does not support any additional TSN features, the focus is restricted to the TAPRIO offered by the OPC UA application. The implementation deploys Xpress Data Path to improve the loopback performance for faster packet processing.

Finally, Denzler et al. [20] focus on the *open62541* OPC UA PubSub stack extension with the 802.1q VLAN tag. It facilitates IEEE 802.1Qbv time-aware scheduling. This work investigates end-to-end timing measures and worst-case execution time analyses, considering various payloads. The experimental setup is distinguished using time-predictable T-CREST platforms hosting the publisher and subscriber with a TSN network handling message transmission. Our work diverges from [20] as we implement our timing analyses using COTS hardware. Furthermore, we expand our scope to cover all Linux TSN queuing disciplines rather than exclusively focusing on IEEE 802.1Qbv time-aware scheduling, thus adding another dimension to our comparative analysis.

The position of this work and the research gap in the existing literature are presented in Table II. We aim to analyze all qdiscs using the same open-source OPC UA software and COTS hardware. This standardized approach enables a fair comparison of qdiscs by subjecting them to identical testing conditions.

TABLE II: Position of our work

Works	[11] [12]	[13]	[14]	[15]	[16] [17]	[18]	[19]	[20]	this work
OPC UA p/s	✓	✓	-	-	-	✓	✓	✓	✓
P2P	✓	✓	-	-	-	-	-	-	✓
Bridge	-	-	✓	✓	✓	-	-	✓	✓
ETF	✓	-	-	-	-	-	-	-	✓
CBS	-	-	-	-	✓	-	-	-	✓
TAPRIO	-	(✓)	✓	✓	✓	✓	✓	✓	✓
COTS HW	✓	-	-	-	-	✓	✓	-	✓
Open-source	✓	?	-	client	-	✓	✓	-	✓

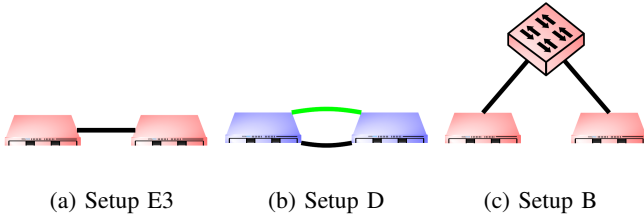


Fig. 6: Test setups with standard hosts (red), powerful hosts (blue), and a dedicated PTP-link (green)

IV. EXPERIMENTAL SETTING

This section describes the setting of the experiments. We outline the measurement setup, including the hardware and software components. This section provides a detailed explanation, ensuring experiments’ repeatability and reliability.

A. Hardware & Software Setup

Our evaluation consists of three setups designed to test different aspects, as illustrated in Figure 6. Figure 6a and Figure 6b represent P2P topologies, with the difference being the inclusion of an additional dedicated link for clock synchronization between the nodes in Figure 6b. This dedicated link is required due to an existing problem of TAPRIO with ETF and PTP [21]. In contrast, Figure 6c depicts the bridged topology.

Table III shows the hardware specifications for each setup. Setups E3 and B rely on the Intel® Xeon® E3-1265L V2 CPU and 16 GB Random-Access Memory (RAM). On the other hand, setup D uses Intel® Xeon® D-1518 CPU with 128 GB RAM. All setups are interconnected with Intel® I210 NIC that supports 1GbE Ethernet and complies with IEEE 802.1AS, IEEE 802.1Qav, and IEEE 802.1Qbv. All selected components are easily accessible and belong to the COTS hardware segment.

To ensure experiment repeatability, nodes use live images that run exclusively in RAM, ensuring that all residual states are erased after each reboot. All hosts run the Linux kernel

TABLE III: Hardware specification of setups E3, B and D

	Setup E3 and B	Setup D
CPU	4C Intel® Xeon® E3-1265L V2	4C Intel® Xeon® D-1518
RAM	16 GB DDR3	128 GB DDR4
NIC	4 × 1 GbE Intel® I210 [†]	6 × 1 GbE Intel® I210 [†]
Motherboard	ASRock Z77E-ITX	Supermicro X10SDV-TP8F

[†]IEEE 802.1Qav, Qbv, AS

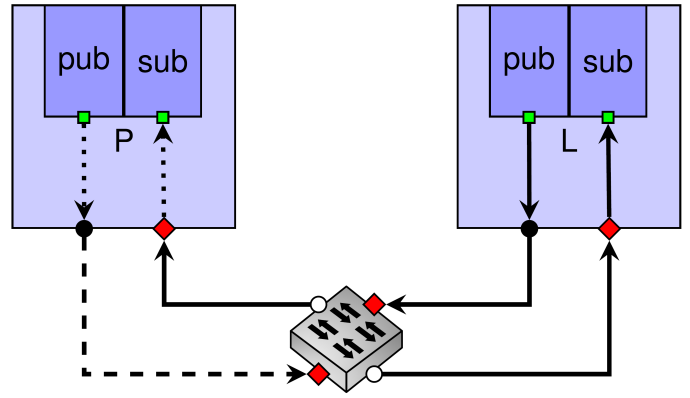


Fig. 7: Measurement points of the bridged topology

5.4.0-45 with an RT-PREEMPT patch, allowing us to use CPU isolation to prevent the system scheduler from placing other tasks on the defined CPU core. To achieve this, we manually set the number of cores not interrupted by other threads. We use the plain orchestration service [22] to orchestrate all experiments.

In the bridged topology, we capture timestamps using *tcpdump*¹¹, which allows for high-precision hardware timestamping if the NIC supports it [23]. Figure 7 shows the measurement points of the software timestamp with the black dots and the hardware timestamp with the red diamonds. We also collect time measurements in the application developed by [11], represented by green squares. However, we find that these timestamps have lower accuracy and thus are not further considered. *tcpdump* records timestamps on the bridge only in the ingress direction. Consequently, we do not include measurements of egress traffic on the bridge. Moreover, we exclude non-solid edges in Figure 7 for the RTT measurement, as they rely on software timestamping, which results in lower precision.

B. PTP Configuration

Our setups rely on the *ptp4l* for time synchronization. This daemon synchronizes the hardware clock of the interface to a GM clock, which ensures accurate and consistent timekeeping across all devices in the network. Once *ptp4l* has synchronized the hardware clock, we use the *phc2sys* tool to synchronize the system clock to the hardware clock. This ensures that our system clock is also accurately synchronized to the GM clock, essential for reliable data transfer and analysis.

In the P2P topology, we configure the publisher host as the GM and the loopback host as a slave. This means that the publisher host is responsible for providing the reference time to the loopback host, which ensures that both hosts are synchronized to the same clock. In the bridged topology, we configure the bridge as the GM and the publisher and loopback hosts as slaves. This ensures that the distance to the next GM clock is a maximum of one hop, which helps to minimize

¹¹<https://www.tcpdump.org/>

latency and maintain accurate timekeeping across all devices in the network [24].

C. Configuration of qdiscs

The most straightforward TSN configuration at the bridge is MQPRIO. It allows for the mapping of desired priorities to class mapping. To maintain consistency throughout the tests, we adopt a uniform mapping where the highest priority is assigned to OPC UA traffic and is mapped to the first hardware queue. All other priorities are treated as BE traffic and are forwarded with the lowest priority.

We use the ETF qdisc in offload mode to leverage the LaunchTime feature of the Intel® I210 NIC. We configure it as the child qdisc of the parent MQPRIO qdisc. This configuration lets us prioritize traffic and effectively manage network resources during data transfer. To ensure the proper functioning of the ETF, we install it following the guidelines provided by the manufacturer.

CBS, similar to ETF, can only be used as a child qdisc and applied to the first two hardware queues on the Intel® I210 NIC. Four specific parameters are required to configure CBS: $idleSlope_x$, $sendSlope_x$, $highCredit_x$, and $lowCredit_x$. These parameters can be set according to the guidelines outlined in the IEEE 802.1Qav standard, as discussed in Section II.

We utilize TAPRIO to classify packets into different traffic classes. To ensure consistency across all hosts, we use a base-time of 1 second and share the same schedule entries. Since the OPC UA application initiates its first cycle at an integer number of seconds, TAPRIO's and its cycles also start simultaneously. Our schedule begins with a BE traffic window, the offset-window, since its duration corresponds to the configurable offset in the OPC UA application. In TxTime-assisted mode, TAPRIO configures a TxTime for each packet using the 0x1 flag. It is accounted for the maximum delay between TAPRIO and the NIC. Additionally, we use ETF-assisted mode, which involves sending packets at precisely the TxTime if a child ETF qdisc with activated offloading is installed for a traffic class. The child ETF qdisc must be configured with skip sock check. Otherwise, ETF would drop packets from TAPRIO.

V. RESULTS

This section presents the results obtained from the experiments. Firstly, we determine the scheduling latency of our hosts, which is the duration between the requested wake-up time of a thread and the actual scheduling by the operating system. Subsequently, we conduct experiments on three different setups: E3 and D, consisting of two hosts connected P2P and B, including a bridge with additional BE traffic. For the P2P setups, we evaluated all available TSN qdiscs, namely MQPRIO, CBS, ETF, and TAPRIO, alongside the default qdisc of Linux, Fair Queuing with Controlled Delay (FQ_CoDel), as a benchmark. We conclude by outlining the potential threats to validity.

TABLE IV: Mean results of ETF with increasing cycledtimes

cycletime [μs]	100	125	150	200	250
d_P [%]	0.029	0.185	0.363	0.037	0.162
d_P (isol) [%]	0.0313	0.0559	0.0092	0.0092	0.0025
d_L [%]	4.93	3.04	0.122	0.126	0.117
d_L (isol) [%]	4.09	2.45	0.0497	0.0481	0.154
d_Σ [%]	4.96	3.22	0.485	0.163	0.279
d_Σ (isol) [%]	4.12	2.51	0.0589	0.0573	0.156
RTT [μs]	195	129	170	246	266
jitter [μs]	10	1.5	0.33	0.528	0.237

A. Experiment Parameters

For each test, we send 700,000 packets and repeat it five times. We evaluate the packet drop rates, RTT, and jitter. We differentiate between d_P and d_L for packet drop rates, representing rates on the publisher and loopback hosts, respectively, and their sum d_Σ . Additionally, for the bridge setup, we represent the drop rates at the bridge to loopback with $d_{b \rightarrow L}$ and to the publisher with $d_{b \rightarrow P}$.

We set up the RT-PREEMPT kernel on all experiment hosts, which results in scheduling latencies between 40 to 130 μs, depending on the setup. To measure the scheduling latency, we run *cyclictest*¹² on the experiment hosts with the publisher thread's priority and the lowest cycle time used in our experiments as the interval. We experiment for 60 s, resulting in the values above. The RT-PREEMPT Linux kernel improves maximum latencies, as evidenced by 7.5 ms and 0.24 ms latencies for setup E3 and D, respectively, when using a regular kernel. We use more conservative values to mitigate the risk of dropping a packet before dequeuing. Table IV shows the impact of cycle time on publisher and loopback hosts with and without central processing unit (CPU) isolation on drop rates, RTT, and jitter. According to the results, 200 and 250 μs values perform the best, considering d_Σ and d_Σ (isol). Our parameter study reveals that selecting a lower cycle time resulted in higher drop rates caused by missing the window opening. In contrast, increasing the cycle time decreases the drop rate and jitter while increasing delay since packets arrive when the window is open and thus do not have to wait for the next window cycle. More conservative 200 and 250 μs values result in higher delays but lower jitter. We select a cycle time of 250 μs since it offers a lower jitter.

Table V shows the drop rate results for offset values ranging from 0 to 250 μs. The drop rate begins at 0.0772 % for zero offset and peaks at 50 μs. Then, the drop rate decreases until it reaches its minimum of 0.0075 % at the offset value of 150 μs. For higher offsets, the drop rate increases again. The mean jitter follows the same trend, with outliers exhibiting multiples of the cycle time $c = 250 \mu s$. These outliers are linked to the subscriber thread missing the timeslot, causing the subsequent packet drop. This behavior is unrelated to sending time precision. Conversely, a 50 μs offset demonstrates the opposite behavior. To ensure consistent behavior, we set the offset value to guarantee that all packets arrive after the

¹²<https://man.archlinux.org/man/cyclictest.8>

TABLE V: Mean results of ETF with increasing offset

offset [μs]	0	50	100	150	200	250
d_P [%]	0.0027	0.0029	0.0058	0.0013	0.0039	0.0078
d_L [%]	0.0745	0.186	0.0327	0.0061	0.0191	0.0722
d_Σ [%]	0.0772	0.187	0.0385	0.0075	0.023	0.08
RTT [μs]	250	500	500	500	500	500
jitter [μs]	0.471	0.844	0.274	0.216	0.265	0.449

TABLE VI: Mean results of ETF with increasing δ

δ [μs]	125	150	175	200	225	250
d_P [%]	0.0028	0.0009	0.0012	0.0023	0.0002	0.0005
d_L [%]	0.0175	0.15	0.0638	0.0077	0.0675	0.0661
d_Σ [%]	0.0203	0.15	0.065	0.01	0.0677	0.0666
RTT [μs]	500	500	500	500	500	500
jitter [μs]	0.245	0.7	0.414	0.221	0.429	0.424

subscriber thread reads new messages. This choice increases latency but reduces the jitter and drop rate. After analyzing the results, we determine that the offset value of 150 μs produces the lowest drop rate, average jitter, and the fewest number of jitter and RTT outliers. Therefore, we fix the offset value to 150 μs for all subsequent experiments.

The next parameter we optimize is the δ value, which must fall within certain upper and lower bounds. Specifically, due to the scheduling latency, we set the lower bound at $\delta > 130 \mu\text{s}$ and the upper bound at the publishing latency $\delta < 0.4c + o = 250 \mu\text{s}$. Our findings indicate that the δ value greater than the publishing latency l_{pub} does not significantly enhance performance. To ensure regular intervals, we conduct measurements in the range of [125, 250] with steps of 25 μs. Table VI shows the results with increasing δ values. The drop rate begins at 0.0203% for $\delta = 125 \mu\text{s}$ and peaks at $\delta = 150 \mu\text{s}$. The drop rate remains constant for higher δ values at around 0.07%. The mean jitter exhibits a similar pattern to the drop rate. Notably, the delta value of 200 μs produces the lowest drop rate, RTT, and jitter values. The RTT remains almost constant at 500 μs and is negligibly affected by δ . Consequently, we set the δ value to 200 μs for all subsequent measurements.

Table VII displays the overview of the parameter selection. All the identified parameters are system-dependent and vary based on the delays caused in the networking stack. δ value is derived from the cycle time and offset. If the CPU is less powerful, the delays could get larger to accommodate the delays caused by the system before the packets reach the NIC.

During our experiments, we utilize UADP over Ethernet. Figure 8 depicts the packet structure with the option to increase the payload in multiples of 9 B.

Our investigation into the impact of packet size on real-time performance is done by publishing 8 B integers with

TABLE VII: Identified optimum parameters

cycle time	CPU isolation	offset	δ
250 μs	on	150 μs	200 μs

8B	14+4B	32B	$n \cdot 9B$	4B	12B
preamble + SoFD	Ethernet	UADP	payload	CRC	IFG

Fig. 8: Frame structure used in the experiments

TABLE VIII: Mean results of ETF with increasing frame sizes

# variables	3	12	30	65	136	163
UADP [B]	59	140	302	617	1256	1499
Link [B]	81	162	324	639	1278	1521
Physical [B]	101	182	344	659	1298	1541
d_P [%]	0.0023	0.0027	0.0021	0.0029	0.0026	0.0045
d_L [%]	0.0077	0.0503	0.0251	0.0603	0.245	25.9
d_Σ [%]	0.01	0.0529	0.0273	0.0631	0.247	25.9
RTT [μs]	500	500	500	501	501	570
jitter [μs]	0.221	0.402	0.304	0.474	0.375	136

1 B UADP overhead in each packet. The first test involves three variables, resulting in a frame size of 81 B. For subsequent tests, we use frame sizes closest to $80 \cdot n$, where $n \in \{1, 2, 4, 8, 16, 32\}$, and a maximum frame size of 1521 B, which is close to the limit of VLAN-tagged Ethernet frames of 1522 B. Table VIII shows the number of published variables, resulting sizes in different layers, as well as ETF results. The drop rate remains below 0.25% for frame sizes up to 1278 B. The publisher host experiences less than 0.005% packet drops, even with maximum-sized frames. However, the loopback host drops a quarter of all maximum-sized frames. This suggests that the OPC UA publisher can handle 1521 B frames and is not the limiting factor. The high drop rates observed in the loopback host may be attributed to longer traversal times and buffering in the networking stack after message reception. Another possibility is that the time required for decoding and storing a received UADP message exceeds a certain threshold. New packets may enter the database at this threshold after the publisher reads from it. In both scenarios, the drop rate comes from the oscillating behavior, where packets sometimes arrive on time and other times arrive too late.

A detailed analysis of the root cause of the poor performance observed with maximum-sized frames would require further experiments and measurement techniques. Additionally, hardware and operating system must provide reliable real-time performance to exclude the impact of factors such as scheduling latencies. However, the observation that all RTT and jitter outliers occur at multiples of the cycle time indicates that the ETF qdisc and Intel® I210 NIC function as intended, sending packets at the scheduled time. Thus, these components are not responsible for the poor performance. Our results show that the maximum payload size that does not result in increased packet drops is 1278 B.

We evaluate the CBS qdisc by testing different levels of over-provisioning and under-provisioning of $idleSlope_x$ values and measuring their impact on the performance. Table IX shows that the drop rate is the lowest at an allocation of 110%. Our findings contrast with IEEE 802.1Qav, which suggests that CBS should limit the flow bandwidth to the $idleSlope_x$.

TABLE IX: Mean results of CBS with increasing $idleSlope_x$

$idleSlope_x$ [%]	80	90	100	110	120
d_P [%]	0.0017	0.0017	0.0017	0.0016	0.0017
d_L [%]	0.129	0.0948	0.137	0.0878	0.0948
d_Σ [%]	0.131	0.0965	0.139	0.0894	0.0965
RTT [μ s]	250	252	251	251	251
jitter [μ s]	1.2	2.13	0.911	0.68	1.1

TABLE X: Mean results of TAPRIO with increasing WS

WS [μ s]	12.5	25	37.5	50	62.5	75
d_P [%]	0.0011	0.0011	0.0005	0.0005	0.0001	0.0001
d_L [%]	0.0044	0.0044	0.0038	0.0039	0.0034	0.0034
d_Σ [%]	0.0055	0.0055	0.0043	0.0044	0.0035	0.0035
RTT [μ s]	500	500	500	500	500	500
jitter [μ s]	0.21	0.21	0.21	0.208	0.208	0.209

The observed behavior is likely due to the CBS qdisc setting the credit to zero when the queue is empty. When a burst of packets enters a CBS queue, the first packet is sent when the credit is non-negative. The credit is then decreased by the $sendSlope_x$ rate and may become negative. If the credit is negative, the next packet in the queue must wait for the credit to increase. This traffic pattern effectively limits the bandwidth to the $idleSlope_x$. However, in our experiment, packets are sent every 250 μ s, leaving roughly a 250 μ s interval where no packet is enqueued. This interval is too long for packets to queue up, resulting in only one packet being in the queue at a time. Consequently, the credit is set back to zero shortly after sending a packet, allowing the next packet to be transmitted immediately. The CBS qdisc of Linux may influence cyclic traffic with shorter cycle times and larger packets. In such cases, the inter-frame gap becomes smaller, and packets start to queue up.

For TAPRIO, we reserve one timeslot for OPC UA traffic and the remaining portion of the cycle for best-effort traffic. We gradually increase the priority timeslot to determine an appropriate duration by 12.5 μ s. At the same time, we reduce the timeslot for best-effort traffic to achieve a cycle time of 250 μ s. Furthermore, the priority traffic is protected by guard bands of 15 μ s before and after its timeslot to prevent interference from other traffic. The guard band duration is chosen to be slightly longer than the serialization time of a maximum-sized 1GbE Ethernet frame. According to Table X, all window sizes (WSs) produce acceptable performance. The mean jitter is 0.2 μ s, and RTT is 500 μ s. The drop rate decreases from 0.0055 % for 12.5 and 15 μ s WS to 0.0035 % for 62.5 and 75 μ s WS. Therefore, a WS of 62.5 μ s is used for the remainder of the experiments.

B. Point-to-Point Topology

We compare the qdiscs in two P2P topologies, E3 and D, equipped with different CPUs. Table XI summarizes the results. The drop rate of the publisher is lower than that of the loopback, and ETF on the publisher causes no packet drops, which validates the parameter selection. However, both TAPRIO and ETF exhibit larger RTT than other qdiscs but

TABLE XI: Comparison of setups E3 and D

qdisc	ETF	FQ_CoDel	MQPRIO	CBS	TAPRIO
E3 d_P [%]	0.0023	0.0017	0.0017	0.0016	N/A
E3 d_L [%]	0.0077	0.0192	0.0939	0.0878	N/A
E3 d_Σ [%]	0.01	0.0209	0.0956	0.0894	N/A
E3 RTT [μ s]	500	250	251	251	N/A
E3 jitter [μ s]	0.221	0.428	0.999	0.680	N/A
D d_P [%]	0	0.0007	0.0007	0.0006	0.0001
D d_L [%]	0.0033	0.0022	0.0026	0.0027	0.0034
D d_Σ [%]	0.0033	0.0031	0.0033	0.0033	0.0035
D RTT [μ s]	500	251	250	250	500
D jitter [μ s]	0.21	13	8.92	10.4	0.209

show less jitter due to precise time control. Additionally, setup D experiences fewer packet drops compared to setup E3.

Figure 9a and Figure 9b depict the Interframe Spacing (IS) for setups E3 and D, respectively. Figure 9a shows an almost constant packet spacing of approximately 250 μ s, as the nearly straight line indicates. However, the plot also shows significant outliers, which could render setup E3 unsuitable for specific real-time applications. In contrast, Figure 9b shows that such outliers are absent for setup D, where the worst deviations are only ± 60 μ s. Consequently, these findings suggest that setup D equipped with a more powerful CPU may be better suited for real-time applications that require more bounded IS. Overall, we see a trade-off between the standard deviation around the average and the worst-case performance.

C. Bridged Topology

The qdiscs are also compared in setup B, as shown in Figure 6c, to investigate further the impact of an additional hop on the performance metrics, building upon the P2P findings. The additional hop is a Linux bridge. We estimate the delay introduced by the bridge by comparing the RTT in setup E3 and setup B. However, a bug in the Linux networking stack prevents us from performing a parallel operation of PTP with TAPRIO and ETF. Thus, the results for this scenario are not available. For the remaining qdiscs, we use the parameters specified in Table VII. In addition, we introduce additional TCP BE cross traffic generated by the *iperf3*¹³ tool. We observe a maximum rate of 940 Mbit/s between the end hosts for all qdiscs, except when ETF is configured, which resulted in a lower rate of 590 Mbit/s. It is worth noting that the BE traffic does not use any shapers but shares the physical interface.

Table XII shows the results when no competing BE traffic exists. The latency caused by the bridge is indicated as l_B . All qdiscs achieve an acceptable drop rate without BE traffic. The best overall drop rate of 0.026 % is achieved with ETF on the end hosts and MQPRIO on the bridge. The second-best results are obtained with FQ_CoDel on all hosts. For all other qdiscs, the drop rate is between 0.14 and 0.18 %. However, the less precise IS may cause the lower performance of CBS and MQPRIO without ETF at the loopback host, as shown in Figure 9c. This explanation does not hold for the

¹³<https://iperf.fr/>

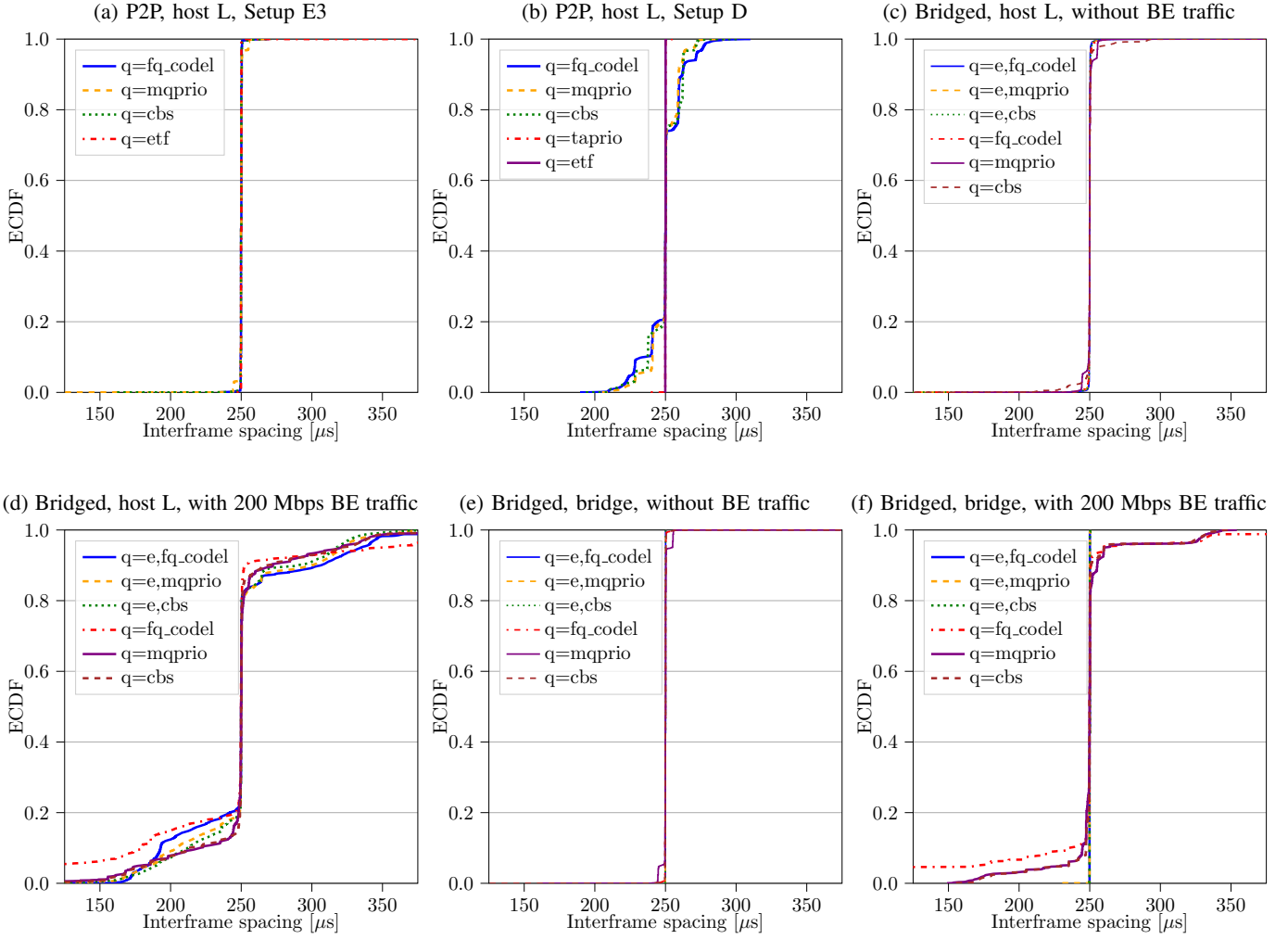


Fig. 9: Comparison of IS of various qdiscs

higher drop rate of ETF on the end hosts and FQ_CoDel or CBS on the bridge, as it shows an almost perfect average behavior in Figure 9e. However, FQ_CoDel or CBS on the bridge and ETF on the end hosts exhibit larger average and median RTT than MQPRIO on the bridge and ETF on the end hosts, leading to more packets missing their time slot for the loopback host’s subscriber, resulting in packet drops. When using BE cross-traffic, all qdiscs exhibit an increased drop rate, as the processing overhead of the cross-traffic affects the other queues despite having a lower priority.

To gain insight into the prioritization of the qdiscs, we compare only the drop rates on the publisher host. Table XIII shows the drop rates, d_P , at different BE traffic rates. Since ETF limits the bandwidth to approximately 590 Mbit/s on the end host, values for higher rates are represented as N/A. The publisher host’s performance is expected to be independent of the qdisc configuration on the bridge. However, we observe no clear drop rate trend for the publisher when using ETF on the hosts. We also see no impact on the drop rate when

TABLE XII: Mean results on setup B without BE traffic

qdisc	E+FQ_C	E+MQP	E+CBS	FQ_C	MQP	CBS
d_P [%]	0.0047	0.0033	0.0018	0.0002	0	0
$d_{b \rightarrow L}$ [%]	0	0.0002	0.0002	0.0007	0.0023	0.0007
d_L [%]	0.171	0.022	0.135	0.054	0.149	0.15
$d_{b \rightarrow P}$ [%]	0.001	0.0002	0.0002	0.0007	0.0007	0.0007
d_Σ [%]	0.176	0.0257	0.137	0.0555	0.151	0.151
RTT [μ s]	547	534	539	280	281	290
l_B [μ s]	47.3	33.8	38.9	29.5	30.4	38.8
jitter [μ s]	2.31	1.06	1.12	0.84	2.25	1.40

increasing the BE traffic volume or using a different qdisc on the bridge. As mentioned earlier, the ETF qdisc drops packets that arrive after their TxTime, indicating a lack of resources. Therefore, we assume that the packet misses the TxTime due to the limited resources, leading to packet drops.

Experiments conducted without ETF show a lower d_P . The CBS qdisc on the publisher host does not drop any packet, regardless of the network load. The same applies to MQPRIO except for the congested network, i.e., at the rate

TABLE XIII: Publisher drop rates, d_P [%], on setup B with increasing BE traffic in [Mbit/s]

qdisc	E+FQ_C	E+MQP	E+CBS	FQ_C	MQP	CBS
0	0.0047	0.0033	0.0018	0.0002	0	0
200	0.0027	0.0023	0	0	0	0
400	0.0017	0.0014	0.0128	0.0003	0	0
600	0.0024	0.0038	0.0025	0	0	0
800	N/A	N/A	N/A	0.0003	0	0
1000	N/A	N/A	N/A	0.0028	0.012	0

of 1000 Mbit/s, where MQPRIO drops 0.012% of packets. FQ_CoDel exhibits a packet drop rate between 0 and 0.0003%, corresponding to two packets being dropped among 700,000 sent packets. In the congested network, FQ_CoDel drops 0.0028%. All qdiscs effectively protect the higher priority traffic, with CBS showing no packet drop and FQ_CoDel and MQPRIO exhibiting no or very low packet drops, except for the congested network. ETF shows the worst drop rate, but the numbers are biased due to the high worst-case scheduling latencies of the hosts in setup B.

The bridge introduces an additional latency overhead ranging from 30 to 47 μ s, which we derive by subtracting the corresponding P2P RTT results from the RTT results of setup B without BE traffic. We observe that RTT's median and mean values in setup B without BE traffic are close, indicating that the outliers do not bias the results. The lowest overhead of 30 μ s is observed for MQPRIO and FQ_CoDel on all hosts. In contrast, using FQ_CoDel only on the bridge and ETF on the end hosts causes the highest overhead of 47 μ s, indicating that FQ_CoDel works best when all hosts use the same qdisc. The overhead of CBS compared to MQPRIO is 5 to 8 μ s. The source of this overhead is unclear and may result from using CBS together with MQPRIO, which adds software component delay. Further detailed analysis is required to investigate this overhead.

The average jitter is between 0.8 and 2.3 μ s, with ETF setups on end hosts achieving smaller jitter, except for FQ_CoDel. The bridge introduces a significant amount of jitter in the presence of BE traffic, but only a few when the network is idle. This is illustrated with IS at the loopback host and the bridge for 0 and 200 Mbit/s network load in Figure 9e and Figure 9f. Figure 9f shows that the IS at the bridge is regular in the loaded network for ETF experiments on the end hosts. After the packets traverse the bridge, they arrive at the loopback host, where more than 20% of the packets have an IS smaller or larger than 250 μ s, as shown in Figure 9d. This holds for all qdisc configurations, including the ETF configured on end hosts. Thus, the sending precision of these setups is lost once the packets leave the bridge.

All setups in the idle network, except for MQPRIO on all hosts, achieve an almost regular IS at the bridge, as depicted in Figure 9e. However, after leaving the bridge, the Empirical Cumulative Distribution Function (ECDF) of IS shows slightly more variance for all experiments, except for CBS on all setups. The CBS experiment shows the least regular IS after leaving the bridge, as shown in Figure 9c.

D. Threats to Validity

In this section, we discuss the limitations of our measurements and setups that may affect the validity of our results. First, the PTP time synchronization used in our experiments is imperfect. While the hardware clocks are regularly adjusted and have a precision within tens of nanoseconds, the system and hardware clock synchronization is less precise, with the two clocks deviating up to 2.7 μ s. Although this bias should be considered when synchronizing the application cycle to a TAPRIO cycle, we do not rely on software timestamps. Hence, this offset is not considered in our measurements. We believe the impact of clock deviations on our measurements is negligible, especially since the bias is small compared to the cycle time used in our experiments. However, it is essential to note that we faced a challenge with PTP and TAPRIO, which required dedicated wiring to synchronize clocks among different nodes [3], [21].

Second, the expressiveness of some experiments may be limited by latency events caused by hardware and the operating system. For instance, single outliers can significantly affect very low drop rates, but it can be challenging to detect such events. We acknowledge that specialized hardware and software offering real-time performance can resolve this issue. However, this approach may also limit the repeatability of experiments by the community. To limit the impact of latency events, we explore real-time kernel possibilities for Linux and increase the number of samples and repetitions. Additionally, we provide the same number of digits for performance parameters to improve the comparability of results in the tables. However, for better readability, we round numbers in the text, which gives a correct impression of the precision of our measurements.

Overall, the results of our experiments using ETF or TAPRIO on all hosts offer a higher precision due to the deterministic sending of the hardware. However, it is crucial to consider the limitations above when interpreting our results.

VI. CONCLUSION

In conclusion, this study examines the real-time performance of OPC UA regarding various qdiscs and their configurations. Drawing on an analysis of related works, we design and conduct experiments to bridge existing research gaps. The results of the experiments are presented and evaluated. The key findings of the study, which correspond to their respective research questions, can be summarized as follows.

Q1, Q2: The presented results demonstrate that synchronous TSN scheduling qdiscs, TAPRIO and ETF, are well-suited for periodic traffic with sub-millisecond cycle times due to their ability to control packet sending times precisely. While the results fall within the use case requirements outlined in the introduction, further hardware and software optimization can reduce the number of outliers, thereby improving worst-case latency and jitter. The remaining qdiscs, MQPRIO, CBS, and FQ_CoDel, exhibit higher jitter but lower RTT than TAPRIO and ETF, indicating they may be better suited for different use cases or scenarios. Ultimately, the choice of qdisc should

be based on the application's specific requirements and the network conditions, considering the trade-offs between them.

Q3: The results of our investigation show that the Linux bridge introduces a two-way latency ranging between 30 and 47 μ s. Such latencies exist with competing BE traffic, dropping no more than 0.004% of packets in the bridged setup while qdiscs prioritize the OPC UA traffic. FQ_CoDel on all hosts achieves the best average RTT overhead, while FQ_CoDel on the bridge and ETF on the end hosts cause the worst average overhead. Our findings demonstrate that IEEE 802.1Qav qdiscs, such as CBS or MQPRIO, are ineffective in limiting the drop rate. However, FQ_CoDel, MQPRIO, and CBS introduce significant jitter in the presence of BE traffic, making them unsuitable for industrial real-time traffic in congested bridged networks. Therefore, a one-hop setup without proper scheduling introduces enough nondeterminism for industrial real-time traffic to make the setup unsuitable. Based on our results, any of the investigated non-TSN qdiscs may be used for the OPC UA PubSub application in a one-directional data transfer scenario, where higher jitter is not a concern.

Q4: For a better qdisc performance, appropriate configuration based on the system's specification and traffic patterns is crucial. For instance, MQPRIO and TAPRIO require mapping of traffic classes to priorities, while CBS requires four additional configuration parameters depending on the traffic pattern used. TAPRIO also configures individual gate schedules and offset settings when used in TxTime-assisted mode. Latencies between hosts can help optimize schedules, and setting the TxTime delay requires information about maximum latencies inside the hardware and software of a host. ETF, which can be used as a child qdisc of MQPRIO or TAPRIO, only requires the configuration of a single value based on maximum latencies inside the host. However, CBS and ETF require at least an additional configuration effort of MQPRIO. Therefore, based on the ascending order of configuration effort, the ranking is FQ_CoDel, MQPRIO, ETF, CBS, and TAPRIO. Following the presented guidelines, users can ensure optimum performance and traffic control with their chosen qdiscs.

The appropriate qdisc configuration is essential in achieving desirable performance, but it is not the only factor. CPU choice also impacts average and worst-case performance significantly. Our results show that setup D, equipped with a powerful CPU, outperforms setup E, equipped with a weaker CPU, in the worst-case scenario. Therefore, if real-time applications are the primary concern, a powerful CPU is the better option due to its lower worst-case latency. Considering qdisc configuration and CPU selection when designing and optimizing networked systems to achieve better performance is essential.

The results of our experiment demonstrate that the implementation of CBS in Linux does not comply with the IEEE 802.1Qav standard. Specifically, when the *idleSlope_x* of a traffic class is set to 80% of the bandwidth, CBS is expected to drop 20% of the packets. However, our findings do not confirm that. As a result, CBS is ineffective in improving the OPC UA PubSub traffic performance with a cycle time

of 250 μ s or more. Based on these results, it is crucial to reconsider using CBS in Linux for traffic management and explore alternative mechanisms that better align with the IEEE 802.1Qav standard.

In conclusion, the findings of this study emphasize the importance of carefully considering the requirements when deploying OPC UA applications. Our research demonstrates that COTS hardware and open-source software can effectively meet the real-time requirements of OPC UA applications. However, it should be noted that the performance of qdiscs varies significantly depending on their configuration. Therefore, it is recommended that system architects and engineers carefully evaluate the characteristics of the qdiscs and configure them according to the specific requirements of the applications. Overall, our research contributes to advancing the understanding of the optimum deployment of OPC UA applications, and our findings aid in developing more efficient and effective OPC UA systems.

REFERENCES

- [1] I. E. Commission, "Opc unified architecture," International Electrotechnical Commission, Tech. Rep., 2020.
- [2] D. Bruckner, M.-P. Stănică, R. Blair, S. Schriegel, S. Kehrer, M. Seewald, and T. Sauter, "An introduction to opc ua tsn for industrial communication systems," *Proceedings of the IEEE*, vol. 107, no. 6, pp. 1121–1131, 2019.
- [3] M. Bosk, F. Rezabek, K. Holzinger, A. G. Marino, A. A. Kane, F. Fons, J. Ott, and G. Carle, "Methodology and infrastructure for tsn-based reproducible network experiments," *IEEE Access*, vol. 10, pp. 109 239–109 239, 2022.
- [4] Y. Lu, L. Yang, S. X. Yang, Q. Hua, A. K. Sangaiah, T. Guo, and K. Yu, "An intelligent deterministic scheduling method for ultra-low latency communication in edge enabled industrial internet of things," *IEEE Transactions on Industrial Informatics*, pp. 1–12, 2022.
- [5] "Ieee standard for a precision clock synchronization protocol for networked measurement and control systems," *IEEE Std 1588-2019 (Revision of IEEE Std 1588-2008)*, pp. 1–499, 2020.
- [6] "Ieee standard for local and metropolitan area networks - virtual bridged local area networks amendment 12: Forwarding and queuing enhancements for time-sensitive streams," *IEEE Std 802.1Qav-2009 (Amendment to IEEE Std 802.1Q-2005)*, pp. C1–72, 2010.
- [7] "Ieee standard for local and metropolitan area networks - bridges and bridged networks - amendment 25: Enhancements for scheduled traffic," *IEEE Std 802.1Qbv-2015 (Amendment to IEEE Std 802.1Q-2014 as amended by IEEE Std 802.1Qca-2015, IEEE Std 802.1Qcd-2015, and IEEE Std 802.1Q-2014/Cor 1-2015)*, pp. 1–57, 2016.
- [8] N. Mühlbauer, E. Kirdan, M.-O. Pahl, and G. Carle, "Open-source opc ua security and scalability," in *2020 25th IEEE International Conference on Emerging Technologies and Factory Automation (ETFA)*, vol. 1, 2020, pp. 262–269.
- [9] N. Mühlbauer, E. Kirdan, M.-O. Pahl, and K. Waedt, "Feature-based comparison of open source opc-ua implementations," 2021.
- [10] "Ieee standard for local and metropolitan area networks—media access control (mac) bridges and virtual bridged local area networks," *IEEE Std 802.1Q-2011 (Revision of IEEE Std 802.1Q-2005)*, pp. 1–1365, 2011.
- [11] J. Pfrommer, A. Ebner, S. Ravikumar, and B. Karunakaran, "Open source opc ua pubsub over tsn for realtime industrial communication," in *2018 IEEE 23rd International Conference on Emerging Technologies and Factory Automation (ETFA)*, vol. 1, 2018, pp. 1087–1090.
- [12] C. Eymüller, J. Hanke, A. Hoffmann, M. Kugelmann, and W. Reif, "Real-time capable opc-ua programs over tsn for distributed industrial control," in *2020 25th IEEE International Conference on Emerging Technologies and Factory Automation (ETFA)*, vol. 1, 2020, pp. 278–285.
- [13] A. Eckhardt and S. Müller, "Analysis of the round trip time of opc ua and tsn based peer-to-peer communication," in *2019 24th IEEE International Conference on Emerging Technologies and Factory Automation (ETFA)*, 2019, pp. 161–167.

- [14] M. H. Farzaneh and A. Knoll, "Time-sensitive networking (tsn): An experimental setup," in *2017 IEEE Vehicular Networking Conference (VNC)*, 2017, pp. 23–26.
- [15] Y. Li, J. Jiang, C. Lee, and S. H. Hong, "Practical implementation of an opc ua tsn communication architecture for a manufacturing system," *IEEE Access*, vol. 8, pp. 200 100–200 111, 2020.
- [16] A. Gogolev, F. Mendoza, and R. Braun, "Tsn-enabled opc ua in field devices," in *2018 IEEE 23rd International Conference on Emerging Technologies and Factory Automation (ETFA)*, vol. 1, 2018, pp. 297–303.
- [17] A. Gogolev, R. Braun, and P. Bauer, "Tsn traffic shaping for opc ua field devices," in *2019 IEEE 17th International Conference on Industrial Informatics (INDIN)*, vol. 1, 2019, pp. 951–956.
- [18] A. Arestova, M. Martin, K.-S. J. Hielscher, and R. German, "A service-oriented real-time communication scheme for autosar adaptive using opc ua and time-sensitive networking," *Sensors*, vol. 21, no. 7, p. 2337, 2021.
- [19] S. Grüner, A. E. Gogolev, and J. Heuschkel, "Towards performance benchmarking of cyclic opc ua pubsub over tsn," in *2022 IEEE 27th International Conference on Emerging Technologies and Factory Automation (ETFA)*, 2022, pp. 1–8.
- [20] P. Denzler, T. Frühwirth, D. Scheuchenstuhl, M. Schoeberl, and W. Kastner, "Timing analysis of tsn-enabled opc ua pubsub," in *2022 IEEE 18th International Conference on Factory Communication Systems (WFCS)*, 2022, pp. 1–8.
- [21] F. Rezabek, M. Bosk, G. Carle, and J. Ott, "Tsn experiments using cots hardware and open-source solutions: Lessons learned," in *2023 IEEE International Conference on Pervasive Computing and Communications Workshops and other Affiliated Events (PerCom Workshops)*, 2023, pp. 466–471.
- [22] S. Gallenmüller, D. Scholz, H. Stubbe, and G. Carle, "The pos framework: A methodology and toolchain for reproducible network experiments," in *Proceedings of the 17th International Conference on emerging Networking EXperiments and Technologies*, 2021, pp. 259–266.
- [23] F. Rezabek, M. Bosk, T. Paul, K. Holzinger, S. Gallenmüller, A. Gonzalez, A. Kane, F. Fons, Z. Haigang, G. Carle *et al.*, "Engine: Flexible research infrastructure for reliable and scalable time sensitive networks," *Journal of Network and Systems Management*, vol. 30, no. 4, p. 74, 2022.
- [24] F. Rezabek, M. Helm, T. Leonhardt, and G. Carle, "Ptp security measures and their impact on synchronization accuracy," in *2022 18th International Conference on Network and Service Management (CNSM)*, 2022, pp. 109–117.